Assessment of dialklyl ketones formation during interesterification of edible oils and fats

Sirine Karra[1]; Alistaire Vionne[1] ; Steven Mascrez[2] ; Giorgia Purcaro[2] ; Véronique Gibon[3] ; Sabine Danthine[1,*]

[1] Food Science and Formulation, University of Liège-Gembloux Agro-Bio Tech, Gembloux, Belgium

[2] Analytical Chemistry, University of Liège- Gembloux Agro-Bio Tech, Gembloux, Belgium

[3] Artemis Lipids by VG, Belgium.

[*] Corresponding Author:

Sabine Danthine, Food Science and Formulation, University of Liège-Gembloux Agro-Bio Tech, Gembloux, Belgium.

Email: sabine.danthine@uliege.be

Author contributions

Sabine Danthine, Alistaire Vionne: Conceived and designed the study. Sirine Karra: Wrote the first draft of the manuscript. Sabine Danthine, Sirine Karra, Alistaire Vionne: Carried out the research. Giorgia Purcaro, Steven Mascrez: analyzed Chromatography data.

All authors contributed to and approved the final draft of the manuscript.

Acknowledgement

The authors would like to thank Sandrino Filocco for his technical assistance.

Funding information

This work was supported by the Fonds de la Recherche Scientifique – FNRS under Grant N° PDR 40014136

Abstract

In view of the nutritional disadvantages of partial hydrogenation (production of unhealthy trans fats) interesterification has emerged to produce suitable fats for trans-free formulations that have improved physicochemical properties. In this context, both chemical (CIE) and enzymatic (EIE) interesterification techniques can be used. However, it has been found that CIE technology may produce process-related by-products known as dialkyl ketones (DAKs). The current study aims at investigating the formation of DAKs during IE. Therefore, five edible oils and fats were selected based on their potential use in IE: Elaeis Guineensis palm oil stearin (POSt), high oleic palm oil stearin (HOPSt), palm kernel oil stearin (PKSt), high oleic sunflower oil (HOSO) and high oleic palm oil (HOPO) and blended. The investigated blends were divided into HOPO-based blends (POSt:HOPO 50:50, PKSt:HOPO 50:50, HPOSt:HOPO 50:50 and 30:70 %w/w) and HOPO-based blends (POSt:HOSO 30:70, 50:50 and 70:30 %w/w). They were all subjected to both CIE (using sodium methoxide as catalyst) and EIE (using TLIM lipase); analyses of physical properties and determination of DAKs content were performed before and after IE. This study demonstrates that DAKs were not formed during the EIE process regardless of the investigated matrix, whereas they were produced during CIE, and that they require sufficient rearrangement of triglycerides (TAG) to be formed. It has also been shown that unsaturated fatty acids are more prone to form DAKs regardless of the fat matrix. However, there is no linear relationship between the amount of DAKs and the amount of unsaturated fat in the matrix.

Keywords:

Interesterification; Dialkylketone; Solid fat content; Fatty acid composition

1. Introduction

Vegetable edible oils are composed of a wide range of triglycerides, which have a major influence on their physical properties and health aspects (Sivakanthan and Madhujith, 2020). Due to their specific chemical composition, their applications in their original form are limited (Sivakanthan and Madhujith, 2020; Lee and Wang, 2022). In addition, they are preferred by consumers over animal oils because they are renewable, of high quality and do not contain cholesterol (Wen et al., 2023). To meet the increasing demand for specific properties of vegetable oils, the industry has actively developed chemical, enzymatic and physical modification technologies to produce fats with precise properties (Gibon, 2012). The best known techniques to extend the use of edible oils in the food industry are blending, fractionation, hydrogenation and interesterification. Regardless of the modification technique used, this leads to changes in the physical and structural properties of the oil (Gibon and Kellens, 2014). Blending of vegetable oils is a simple and widely accepted practice in the industry that enables the production of new products with the desired physiochemical properties. However, the effectiveness of blending depends on the chemical composition of the oils used as raw materials (Lee and Wang, 2022). Fractionation or fractional crystallization is an important physical modification technique used by the industry to improve the application of oils (Lee and Wang, 2022; Gibon, 2012). It is a cost-effective, safe and environmentally friendly method compared to other edible oil processing technologies (Gibon, 2012). Hydrogenation is a chemical process utilized to modify liquid lipids, converting them into solid or semi-solid fats and enhancing their oxidative stability (Zbikowska et al., 2023). While partially hydrogenated fats possess favorable properties for numerous food products, they also contain significant levels of trans fatty acids (TFAs) resulting from the conversion of cis-fatty acids into trans-fatty acids during the process (Zbikowska et al., 2023; Lee and Wang, 2022; Gibon, 2012). The consumption of partially hydrogenated fats has been associated with an

elevated risk of cardiovascular issues (Mozaffarian et al., 2009) and par tially hydrogenated oils are now banned from the food industry. The interesterification (IE) process involves modifying oils by rearranging the fatty acid moieties within or between triacylglycerols (TAGs). This results in a product with different properties suitable for various food applications (Danthine et al., 2022; Sivakanthan and Madhujith, 2020; Santoro et al., 2018). IE can produce structured lipids with zero TFAs, making them valuable for replacing partially hydrogenated fats in products such as margarines and shortenings (Danthine et al., 2022; Sivakanthan and Madhujith, 2020). As the demand for trans-free fat alternatives grows, the interesterified fats market is still expected to expand (Sivakanthan and Madhujith, 2020). The interesterification process can be carried out using either chemical catalysts (chemical interesterification) or biological catalysts such as lipases (enzymatic interesterification) (Gibon, 2012). Chemical interesterification (CIE) is a process that induces the random rearrangement of acyl groups within TAGs (Gibon and Kellens, 2014; Lee and Wang, 2022). CIE typically utilizes a catalyst but can also be conducted without, but at very high temperatures (Rousseau et al., 2017). The utilization of a catalyst diminishes the reaction time and temperature (Gibon and Kellens, 2014; Rousseau et al., 2017). Sodium methoxide serves as the predominant catalyst, although NaOH was previously utilized (Gibon and Kellens, 2014; Rousseau et al., 2017). It is important to emphasize that catalysts can react with moisture, free fatty acids (FFA), and peroxides present in the oil (Dijkstra, 2015). Consequently, the quality of the oil and the effectiveness of the drying system significantly influence the necessary amount of catalyst (Gibon and Kellens, 2014). On the other hand, enzymatic interesterification (EIE) is increasingly recognized as a promising technique for modifying lipids, driven by the growing recognition of the nutritional advantages of fats and the goal of eliminating organic solvents and chemicals in fat and oil modifications (Lee and Wang, 2022; Gibon and Kellens, 2014). EIE presents some advantages over CIE and has been adopted across various industries, including to produce cocoa butter

equivalents and human milk fat substitutes (Gibon and Kellens, 2014). Furthermore, it facilitates the creation of healthier products to meet the demand for trans-fat-free base-stocks in spreads, margarines, and confectionery fats (Rousseau et al., 2017). In comparison to CIE, EIE employs specific and reusable enzymes, and operates under milder reaction conditions (Sivakanthan and Madhujith, 2020; Zbikowska et al., 2023). Secondary reaction products, commonly referred to as Dialkyl Ketones (DAKs), have been identified and associated with the chemical process (Danthine et al., 2022; Santoro et al., 2018). DAKs have been detected in the unsaponifiable portion of chemically interesterified oils and have garnered attention. Currently, a precautionary approach is taken with respect to DAKs due to a potential hazard, but no specific regulations have been implemented regarding their presence in food. Even if further research is necessary to comprehend the health implications of DAKs, assessing the extent of their formation upon IE reaction worths to be investigated (Danthine et al., 2022).

In this context, this study investigates CIE and EIE in a randomized TAG rearrangement process within mixtures of edible vegetable oils. Thus, several edible oils and fats were selected according to different criteria, e.g. their potential use in IE (a hard fat combined with a softer fat), their classification as "new fats" (sunflower and palm oil with high oleic acid content) and their relative proportion (to emphasize the possible influence of the degree of unsaturation). The primary focus is to evaluate the DAKs content in all the blends after the two types of IE and comprehend how the fat matrix composition influences their production.

2. Experimental Procedures

2.1.Samples

Palm oil stearin (POSt) was received from Fuji Oil Europe (Ghent, Belgium), while high oleic palm oil (HOPO), high oleic palm oil stearin (HOPOSt), palm kernel oil stearin (PKSt) and high oleic sunflower oil (HOSO) were kindly provided by Daabon S.A.S (Santa Marta,

Colombia).These edible oils have been selected to produce HOSO- and HOPO-based blends, namely: POSt:HOSO (50:50 w:w%), POSt:HOSO (30:70 w:w%), POSt:HOSO (70:30 w:w%), POSt:HOPO (50:50 w:w%), HOPSt:HOPO (50:50 w:w%), HOPSt:HOPO (30:70 w:w%) and PKSt :HOPO (50:50 w:w%).

2.2.Reagents and catalysts

Ethanol 96%, diethyl ether, methanol, chloroform stabilized with about 0.6% of ethanol, KOH in ethanol (0.1 N), sodium thiosulfate in aqueous solution, glacial acetic acid (99-100%), potassium iodine, n-hexane, phenolphthalein (1% in ethanol), 2,2,4-Trimethylpentha and standards of 14-heptacosone were purchased from VWR Chemicals. The bleaching earth (Tonsil Optimum 210FF) was from Clariant Products (GmbH) and the *p*-Anisidine for synthesis was purchased from Sigma-Aldrich (St. Louis, MO). The chemical catalyst, sodium methoxide (98%), was purchased from Thermo Scientific (Kandel, Gmbh). The enzymatic biocatalyst, Lipozyme® TL IM from *Thermomyces lanuginosus*, was kindly provided by Novozymes A/S (Bagsvaerd, Denmark).

2.3.Methods

2.3.1. Chemical Interesterification (CIE)

Each fat blend (500 g) was first dried for 1 hour at 90°C under vacuum (±25 mbar). Sodium methoxide was then added (0.1%, w/w) and the mixture was homogenized (1 minute at 16,000 rpm), using an Ultra-Turrax T25 (IKA Co., Germany). The pear-shaped flask was then reconnected to the Rotavapor (Buchi, Germany) and heated for 30 minutes at 90°C under vacuum (± 25 mbar). After 30 minutes, the flask was disconnected and an excess stoichiometric amount of 20% (w/w) citric acid was added to inactivate the catalyst.Post-bleaching was performed at 90°C, ± 25 mbar, for 30 minutes. Finally, the entire content was filtered through

a preheated Buchner filter, using a Whatman paper No. 1 (De Clercq et al., 2012). After filtering, the CIE oil was quickly placed under dark, at 4°C for storage until analysis.

2.3.2. Enzymatic interesterification (EIE)

The fresh Lipozyme® TL IM was used as catalyst and was first deaerated and dehydrated as recommended by the supplier. The batch-EIE was conducted during 24h at a lab-scale using a double jacketed reactor as described by Danthine et al., (2022). After the designated reaction time, stirring was stopped and the oil was recovered by vacuum filtration using a Wathman paper No. 1 and a Büchner funnel.

2.3.3. Oil quality

Five quality criteria were investigated following specific protocols according to the Official Methods of Analysis of the American Oil Chemists' Society (AOCS, 2009): peroxide value (AOCS Cd8 - 53), FFA content (AOCS Ca5a - 40), pH of water extract, moisture content (AOCS Ca 2c-25) and p-anisidine value (AOCS Cd18 - 90).

2.3.4. FA composition

The fatty acid (FA) composition was analyzed using a Trace GC Ultra gas chromatograph (GC; Thermo Fisher Scientific, Belgium) equipped with a flame ionization detector (FID), as described by Kouassi et al., (2023). FA methyl esters were prepared following the AOCS Ce 2-66 method and analyzed in GC-FID using a Stabliwax DA column measuring 30 m in length, 0.25 μm in thickness, and 0.25 μm in diameter. Injection was carried out in splitless mode (with a splitless time of 0.85 min) at 250°C. Helium was employed as the carrier gas at a constant flow rate of 1 mL/min. The temperature program was as follows: an initial hold at 50°C for 1 min, followed by an increase to 150°C at a rate of 30°C/min, and then to 240°C (with a hold

for 10 min) at 5°C/min. The FID was set at 250°C. The identification of FA methyl esters was accomplished by comparing their retention times with those of pure reference.

2.3.5. SFC analysis

The SFC melting profiles were used to evaluate the interesterification reactions, as it is a standard practice on an industrial scale (De Clercq et al., 2012). The profiles were determined on the different fat blends using a p-NMR spectrometer (Minispec-mq20, Bruker, Karlsruhe, Germany) according to the IUPAC2.150 serial method (1 h at 0 °C, 30 min at each temperature) (IUPAC, 1987). All SFC analyses were performed in duplicate.

2.3.6. DAKs analysis

The DAK content was determined according to the method described by Mascrez et al., (2021). For this analysis, the microwave-assisted saponification method (MAS) was used with an Ethos-X microwave system equipped with a high-pressure rotor SR 12 from Milestone Srl (Milan, Italy). In brief, in the MAS method, the sample is rapidly heated to a temperature of 90°C within 2 minutes at a power of 800 W. The temperature is maintained for 10 minutes with continuous magnetic stirring, then the samples are cooled to 60°C. Subsequently, the unsaponifiable fraction was collected using a lab-made solid phase extraction (SPE) column to isolate DAK from the remaining fat components. Finally, GC-FID (Thermo Fischer Trace Ultra 1300) and GC-MS (Shimadzu GCMS-TQ8050 NX,) were used for quantification and identification, respectively.

2.3.7. Data analysis

All experiments were carried out either in triplicate or in duplicate. Chemical and enzymatic interesterification was performed in duplicate for each blend. Then DAKs were performed in duplicate for each reaction replicate. Results were analyzed using Fisher-Snedecor test and

Student's t-test with least significant difference at 95% confidence interval. All statistical analyses were performed using R-4.3.1 software.

3. Results and discussion

3.1. Oil quality

The quality of the oil plays a decisive role in the effectiveness of both the chemical and enzymatic catalysts used for IE (Dijkstra, 2015). All parameters were checked and met the oil quality requirements for industrial scale use, with the following target values (peroxide value: 3 meq O_2/kg, FFA content: <0.1%, pH of the water extract: >6, moisture content: ≤ 0.05% and p-anisidine value: <10) (Gibon and Kellens, 2014).

3.2.Fatty Acid composition (FAC)

The fatty acid composition of oil blends is important as it is closely related to both the nutritional and organoleptic properties of fats. Furthermore, this analysis is of great importance to help with formulating new healthy foods (Danthine et al., 2022). The results regarding the FA of HOSO- and HOPO-based blends are shown in Table 1. As expected, the results show that four fatty acids predominate in all blends tested, namely palmitic acid (P), stearic acid (S), oleic acid (O) and linoleic acid (L) (C16:0, C18:0, C18:1 and C18:2, respectively) and that lauric acid (La) (C12:0) predominate in the blend consisted with palm kernel oil stearin (PKSt:HOPO, 50:50). The other fatty acids are considered as minor ones. This analysis was namely carried out to correlate the amount of produced DAK with the unsaturation degree of the blends (un-saturated fatty acid (UnSAFA) percentages).

3.2.1. HOSO-based blends

As can be seen in Table 1, the reduction in the proportion of HOSO led to an increase in C16:0 and a decrease in C18:0, C18:1 and C18:2, with C18:1 playing a greater role. These results

were expected, as according to the literature, POSt is rich in palmitic acid (Soares et al., 2009; Tan and Nehdi, 2012) and HOSO is rich in oleic acid (Grompone, 2020; Morselli Ribeiro et al., 2017).

3.2.2. HOPO-based blends

For the HOPO-based blends, Table 1 shows that the decrease in HOPO compared to HPOSt leads to an increase in palmitic acid and a decrease in both oleic and linoleic acids. This trend was expected due to the richness of HOPO in C18:1 and HPOSt in C16 (Cedeno-Sanchez et al., 2023). Mixtures consisting of 50% HOPO show that PKSt:HOPO has the lowest values in C16, C18, C18:1 and C18:2, which is due to the lack of PKSt in these FA (Ornla-ied et al., 2021; Borhan et al., 2011). For both HPOSt and POSt mixed with 50% HOPO, the results show that HPOSt:HOPO is richer in C18:1 and lower in C16 than POSt:HOPO, which is expected according to the literature (Cedeno-Sanchez et al., 2023; Ramli et al., 2008).

POSt and HOPO have similarities in the types of FAs but differ in proportion. They both have a high content of palmitic acid and oleic acid, but HOPO has a higher content of oleic acid and a lower content of palmitic acid than POSt. In fact, the POSt edible oil, in addition to being a conventional oil, has been fractionated to obtain stearin. PKSt, for its part, stands out completely from the selection because it is a lauric fat, which means that it consists mainly of lauric fatty acid (Laning, 1985; Ornla-ied et al., 2021; Ornla-ied et al., 2022). The other main component is myristic acid.

3.3.Melting properties: SFC analysis

All investigated blends were analyzed for their SFC profile before and after IE. Indeed, to characterize edible fats, it is important to evaluate their melting profiles and melting points. As reported by Karabulut et al., (2004), many properties such as general appearance, ease of

packaging, organoleptic properties, spreadability and oil separation are related to the amount of fat crystals and the SFC profile which is an important parameter to assess the suitability of fats for a specific application (Danthine et al., 2022).

Two profiles were generated for each interesterification reaction, as each interesterification (CIE and EIE) was performed in duplicate. If there was no significant difference between the data of the two curves obtained for each type of interesterification, an average curve was plotted. Furthermore, it was noted that the profiles of the CIE and EIE blends were identical; as a result, for clarity only the CIE blends are shown (Figures 1 and 2).

3.3.1. HOSO-based blends

Figure 1 illustrates the SFC profiles of all interesterified (IE) and non-interesterified (NIE) blends composed by HOSO including POSt:HOSO (30:70 (a) ; 50:50 (b) ; and 70:30 (c) w:w%) and shows a remarkable change in the melting profile obtained before and after interesterification for each of them.

The melting points of all blends are significantly lower than those of their non-interesterified counterparts. As the proportion of POSt in the blend increases, the difference between the melting points of IE and NIE blends decreases. These discrepancies are 20, 10 and 5°C for POSt:HOSO (30:70, 50:50, 70:30) blends, respectively.

The ΔSFC represents the difference in solid fat content value at each temperature between IE and NIE Blends. The Figure 1 shows that the largest ΔSFC are observed at higher temperatures as the proportion of POSt in the blend increases. In addition, the differences in the SFC profiles from 5 to 20°C are more prominent with lower proportions of POSt in the blend. This phenomenon can be attributed to the formation of di-unsaturated triglycerides (SUU). Their

increased occurrence explains the sharp decrease in SFC content in the temperature range of 5 to 20°C (Zhang et al., 2021).

Increasing the POSt content in the blend also leads to an increase in temperature at which the IE blend becomes softer than the non-IE blend. For the POSt:HOSO (30:70), (50:50) and (70:30) blends, the IE blend exhibits greater hardness from 0 to 5°C, 0 to 10°C and 0 to 15°C, respectively, transitioning to a softer behavior after the crossing points between IE and NIE blends at 5, 10 and 15°C, respectively. This trend could be due to an increase in SUU with increasing POSt content. The increase in POSt content can also explain the greater decrease in the slope of the curve between 5 and 20°C.

3.3.2. HOPO-based blends

Figure 2 illustrates the SFC profiles of all interesterified (IE) and non-interesterified (NIE) blends composed with HOPO namely HOPSt/HOPO (30:70 %) (a), HOPSt/HOPO (50:50 %) (b), POSt:HOPO (50:50 w:w%) (c), PKSt/HOPO (50:50%) (d).

As can be seen, contrarily to previous blends containing 50% HOSO, there are only few changes in the SFC profile of the four blends containing 50% HOPO after interesterification. Nevertheless, the POSt:HOPO (50:50 w:w%) CIE and EIE blends show the greatest change in their SFC profile due to IE (Figure 2.c). In fact, they show lower SFC profiles after 30°C and harder below 30°C compared to the NIE blend. Regarding the HOPSt:HOPO 30:70 w:w % blend, the results show that the SFC profiles of the EIE and CIE fats are more distinct compared to the initial NIE blend than those of the HOPSt:HOPO (50:50 w:w%) blend before and after IE (Figure 2).

The blends consisting of HOSO show large changes in their SFC profiles after IE, in contrast to HOPO-based blends that do not exhibit this property. This trend can be attributed to the TAG

279 composition. The closer the TAG composition is to the random situation, the smaller the
280 change in the SFC profile. Indeed, the TAG composition of blends containing 50% HOPO
281 approaches equilibrium (data not shown), which explain the small changes observed in the SFC
282 melting profile after IE.

283 3.3.3. Quantification of the IE impact on the physical properties of the blends

284 It was important to quantify how the IE process affected the blends' physical properties
285 (measured by SFC profiles in the current study). Consequently, a parameter called the "Δ area"
286 metric was computed to quantify and compare these impacts. Indeed, the “Δ Area” represents
287 the difference between the areas under the melting curves obtained respectively for IE and NIE
288 blends. This parameter was determined as it provides an estimate of the rearrangement rate of
289 acyl groups within TAGs. Accordingly, the rearrangement was very low when there is a small
290 Δ area. Thereby, it was remarkable for HOSO-based blends that total Δ Area was larger when
291 POSt increases in the blend, which was also reflected in a pronounced shift in the SFC profiles.
292 Regarding POSt: HOPO (50:50 w:w%), the change in SFC profiles after IE were quite weak.
293 As Figure 2 shows, the largest difference (Δ SFC) was observed for each blend in the range
294 from 0 to 15°C. It appears that the changes in all blends was due to a slight increase in SUU
295 content compared to UUU content (data not shown). In the case of the HOPSt:HOPO (30:70
296 w:w%) blend, the change in the “total Δ area" expressing the cumulative difference alongside
297 the SFC profile between NIE and IE is almost twice more important compared to the 50-50%
298 blend (Table 3).

299 3.4.DAK analysis

300 3.4.1. HOSO-based blends

301 All samples, NIE, EIE and CIE were analyzed for their DAKs content. Results are presented
302 in Table 2. As each interesterification reaction was performed in duplicates and each DAKs

analysis was also performed in duplicates, an equality of variance test followed by a Student's t-test were performed between the results obtained for the reaction duplicates. If there were no significant differences between the duplicates, their results were combined. In all cases, the results showed that the NIE were free of DAKs and that none of the EIE reactions lead to the formation of DAKs (Table 2 and 3). On the contrary, DAKs were measured in most of the samples after CIE. Table 2 shows the results in terms of DAKs content and composition for each POSt:HOSO-based blend before and after interesterification (CIE-EIE). Contrarily to EIE, DAKs were identified in the three blends after CIE and C16:0 – C16:0, C16:0 – C18:1 and C18:1 – C18:1 were identified and quantified. The identified DAKs species are consistent with the FAC of the two fats involved in the three blends. The POSt:HOSO 50:50 blend showed significant differences in DAKs species compared to both POSt 30:70 and 70:30 blends (< t-value). Similarly, the POSt:HOSO 30:70 and 70:30 blends showed significant differences in terms of total DAKs content, C18:1-C18:1 and C16:0-C16:0 formation. However, there was no significant difference in the amount of C16:0-C18:1 between these two blends. Significant differences in C16:0-C18:1 formation were seen between the 30:70, 70:30 blends and the 50:50 blend. This suggests that when one of the materials, POSt or HOSO, dominates the mixture, a level of DAKs is formed consisting of the two main fatty acids that compose the mixture (i.e. C16 and C18:1 in this case). Meanwhile, the highest DAKs levels are predominantly formed by the fatty acid that is most abundant in the blend, resulting in symmetrical DAKs forms. This is supported by the fact that only the blend with the highest palmitic acid content leads to the production of C16:0-C16:0 DAKs after chemical interesterification. Likewise, for the blend POSt:HOSO (30:70 w:w%) containing the largest amount of C18:1, it presents the highest C18:1 – C18:1 content after CIE.

Relating to the previous findings for SFC data (section 3.3), it was obvious that there is a correlation between the extent of change in the SFC profile after IE and the amount and

diversity of DAKs produced. It was found that larger shifts in the SFC profile are associated with a wider range of DAKs species. However, increasing DAKs diversity does not necessarily indicate a higher overall DAKs content (Table 2). This intricate relationship emphasizes the complexity of DAKs formation in response to different blend compositions (Figure 3).

Furthermore, Danthine et al., (2022) reported that the formation of DAKs could be related to the content of unsaturated fats in the matrix. However, in this case while the highest unsaturated blend has the highest DAKs content, the second highest content comes from the least unsaturated blend. This implies that the generation of DAKs is not proportional to the unsaturated fats in the matrix. It suggests a closer relationship between DAKs formation and the extent of TAG rearrangement, which depends on the formation of enolate anions. Indeed, the formation of DAKs involves a concurrent reaction, which includes a β-keto ester species serving as an intermediate in the enolate reaction during interesterification (Santoro et al., 2018; Lestido-Cardama et al., 2020). The process leading to DAK creation has been of interest since earlier research by Sprague et al., (1934) on Claisen condensation and diketone formation. Initially, sodium methoxide abstracts a hydrogen from the α-carbon of the carbonyl group, forming the enolate anion, which is stabilized through resonance. DAKs are comprised of a central carbonyl group bordered by two aliphatic chains. These chains, ranging from C10 to C24, stem from the original fatty acids involved in the decarboxylation process (Danthine et al., 2022; Santoro et al., 2018). Therefore, the hypothesize is that if there are no or only minor changes in the SFC profile, the enolate anion is not formed or only in very small amounts, which means that the concomitant reaction is less “promoted” and therefore fewer or no DAKs are formed.

Our results show that a high proportion of unsaturated fats in the blend lead to larger amounts of DAKs after CIE. However, when highly saturated blends undergo significant changes in

SFC profile after CIE, their total DAKs content increases (albeit lower than blends high in unsaturated fatty acids). This amount is higher than for the same blend consisting of a balanced ratio of unsaturated and saturated fats (i.e. 50:50 w:w%). Moreover, unsaturated fatty acids (UNSAFA) tend to form more symmetrical DAKs than SAFA. Symmetrical SAFA-based DAKs only occur when the SAFA is dominant in the fat matrix. Conversely, symmetrical DAKs with UNSAFA composition occur in all blends, corresponding to the different C18:1-C18:1 amount (see Table 2).

3.4.2. HOPO- based blends

The following Table 3 shows the results in terms of DAKs profiles of each sample. As in the previous blends, no DAKs were detected neither in NIE nor in EIE samples. Moreover, contrarily to what was observed in the previous blend, DAKs were not identified in most CIE samples. This is linked with minimal changes in the SFC profile. Only POSt:HOPO (50:50 w:w%) and HOPSt:HOPO (30:70 w:w%) present after chemical interesterification the following DAK species: C16:0 – C16:0, C16:0 – C18:1 and C18:1 – C18:1, which were the same species as previously identified in the CIE HOSO-based blends. This indicates that DAKs are formed only if and when a certain level of matrix rearrangement is reached. This assumption is supported by the fact that no DAKs were formed in the HOPSt:HOPO blend (50:50 w:w%), whereas they were formed at the 30:70 w:w% ratio.

In terms of total Δ Area, the PKSt:HOPO (50:50 w:w%) and HOPSt:HOPO (50:50 w:w%) blends have lower values (62 and 46, respectively) than HOPSt:HOPO (30:70 w:w%) and POSt:HOPO (50:50 w:w%) blends (78 and 136, respectively), which was in accordance with the obtained results as no DAKs, including those consisting of lauric fatty acids, were produced for the first two mixtures. This suggests the possibility of a matrix-specific rearrangement threshold that must be exceeded to trigger the formation of DAKs.

In addition, the DAKs profile of POSt:HOPO (50:50 w:w%) is comparable to that of POSt:HOSO (70:30 w:w%) in terms of generated DAK species. However, the main difference between them lies in the amounts of each DAKs species produced as POSt:HOSO (70:30 w:w%) yields higher levels of DAKs than POSt:HOPO (50:50 w:w%). This phenomenon can be attributed to the FAC of the blend. The POSt:HOSO (70:30 w:w%) blend contains a higher proportion of UNSAFA. This correlation suggests that a higher proportion of UNSAFA in the fat matrix could contribute to an increased formation of DAKs.

In summary, the composition of the matrix undergoing interesterification significantly influences the types of DAKs formed. It was proved that when the TAG composition of the matrix approaches random equilibrium, fewer DAKs are formed, which may be probably due to the limited formation of enolate anions. Furthermore, the effect of the UNSAFA content in the material to be interesterified is more complex than a simple linear increase in DAKs at higher UNSAFA content. Interestingly, symmetric DAKs consisting of UNSAFA seem to form more easily than their saturated counterparts.

4. Conclusion

In conclusion, the study of interesterification processes using mixtures of edible vegetable oils has provided valuable insights into the formation of DAKs. The results of this study shed light on the intricate relationships between the composition of the fat matrix and the resulting content of DAKs. One of the most important observations is the clear distinction between EIE and CIE in relation to the formation of DAKs. It was consistently observed that DAKs were absent when EIE was performed, regardless of the composition of the fat matrix. Furthermore, DAKs are closely associated with the FAC of the fat matrix. The specific types of DAKs that are formed show a direct dependence on the presence and proportion of different fatty acids in the matrix. In particular, unsaturated fatty acids appeared to play a more important role in the formation of

DAKs than their saturated counterparts. This suggests a preferential involvement of unsaturated fatty acids in the reaction pathways leading to DAKs. Nevertheless, the relationship between the amount of unsaturated fat in the matrix and the formation of DAKs (total amount) was found to be non-linear. This suggests that the formation of DAKs is influenced by a complex interplay of factors beyond the simple degree of unsaturation. The study supports the assumption that the degree of randomness in TAG composition influences the formation of DAKs. An initially more random TAG distribution resulted in fewer DAKs during CIE, consistent with the critical role of enolate anions in the interesterification process.

While this study revealed the presence of DAKs in the CIE samples and their dependence on material composition and quality, research into the effects of different CIE parameters (temperature, time, catalyst concentration) on the formation of DAKs remains valuable.

References

AOCS, A. O. C. S. 2009. "Official methods and recommended practices of the AOCS." In.: AOCS Denver.

Borhan, R.-H., Said, M., & Sahri, M. M. (2011). Enzymatic interesterification of palm products for producing low calorie cocoa butter substitutes. Journal of Applied Sciences, 11:3750-3754,

Cedeno-Sanchez, V., Perez-Santana, M., Mehta, D., Godinez, S., Gu, L., Miller, V. M., & MacIntosh, A. J. (2023). Thermomechanical Properties of High Oleic Palm Oil Assessed Using Differential Scanning Calorimetry, Texture Analysis, Microscopy, and Shear Rheology. Gels, 9:798,

Danthine, S., Closset, S., Maes, J., Mascrez, S., Blecker, C., Purcaro, G., & Gibon, V. (2022). Enzymatic interesterification to produce zero-trans and dialkylketones-free fats from rapeseed oil. OCL, 29:36,

De Clercq, N., Danthine, S., Nguyen, M. T., Gibon, V., & Dewettinck, K. (2012). Enzymatic interesterification of palm oil and fractions: monitoring the degree of interesterification using different methods. Journal of the American oil chemists' society, 89:219-229,

Dijkstra, A. J. (2015). Interesterification, chemical or enzymatic catalysis. Lipid Technology, 27:134-136,

Gibon, V. (2012). 'Palm oil and palm kernel oil refining and fractionation technology.' In, *Palm oil* (pp. 329-375). Elsevier.

Gibon, V., & Kellens, M. (2014). 'Latest developments in chemical and enzymatic interesterification for commodity oils and specialty fats.' In, *Trans fats replacement solutions* (pp. 153-185). Elsevier.

Grompone, M. A. (2020). 'Sunflower and High-Oleic Sunflower Oils.' In, *Bailey's Industrial Oil and Fat Products* (pp. 1-54).

Karabulut, I., Turan, S., & Ergin, G. (2004). Effects of chemical interesterification on solid fat content and slip melting point of fat/oil blends. European Food Research and Technology, 218:224-229,

Kouassi, A. K., Alabi, T., Cissé, M., Purcaro, G., Moret, S., Moret, E., . . . Danthine, S. (2023). Assessment of composition, color, and oxidative stability of mango (Mangifera indica L.) kernel fats from various Ivorian varieties. Journal of the American Oil Chemists' Society,

Laning, S. J. (1985). Chemical interesterification of palm, palm kernel and coconut oils. Journal of the American Oil Chemists' Society, 62:400-407,

Lee, W. J., & Wang, Y. (2022). 'Blending, Hydrogenation Hydrogenation, Fractionation Fractionations and Interesterification Interesterification Processing.' In, *Recent Advances in Edible Fats and Oils Technology: Processing, Health Implications, Economic and Environmental Impact* (pp. 189-234). Springer.

Lestido-Cardama, A., Störmer, Á., & Franz, R. (2020). Dialkylketones in paperboard food contact materials—method of analysis in fatty foods and comparative migration into liquid simulants versus foodstuffs. Molecules, 25:915,

Mascrez, S., Danthine, S., & Purcaro, G. (2021). Microwave-assisted saponification method followed by solid-phase extraction for the characterization of sterols and dialkyl Ketones in fats. Foods, 10:445,

Morselli Ribeiro, M. D., Ming, C. C., Silvestre, I. M., Grimaldi, R., & Ap. G. Gonçalves, L. (2017). Comparison between enzymatic and chemical interesterification of high oleic sunflower oil and fully hydrogenated soybean oil. European Journal of Lipid Science and Technology, 119:1500473,

Mozaffarian, D., Aro, A., & Willett, W. C. (2009). Health effects of trans-fatty acids: experimental and observational evidence. European journal of clinical nutrition, 63:S5-S21,

Ornla-ied, P., Podchong, P., & Sonwai, S. (2022). Synthesis of cocoa butter alternatives from palm kernel stearin, coconut oil and fully hydrogenated palm stearin blends by chemical interesterification. Journal of the Science of Food and Agriculture, 102:1619-1627,

Ornla-ied, P., Tan, C. P., Wang, Y., & Sonwai, S. (2021). Cocoa butter alternatives from enzymatic interesterification of palm kernel stearin, coconut oil, and fully hydrogenated palm stearin blends. Journal of the American Oil Chemists' Society, 98:53-64,

Ramli, M. R., Lin, S. W., Yoo, C. K., Idris, N. A., & Sahri, M. M. (2008). Physico-chemical properties and performance of high oleic and palm-based shortenings. Journal of oleo science, 57:605-612,

Rousseau, D., Ghazani, S., & Marangoni, A. 2017. "12 Chemical Interesterification of Food Lipids: Chemistry, Nutrition, and Biotechnology." In, 349. CRC Press Boca Raton, FL.

Santoro, V., Baiocchi, C., Dal Bello, F., Gastaldi, D., Aigotti, R., Zorzi, M., . . . Magni, M. (2018). Formation of by-products during chemical interesterification of lipids. Detection and characterization of dialkyl ketones by non-aqueous reversed-phase liquid chromatography-high resolution mass spectrometry and gas chromatography-mass spectrometry. Journal of Chromatography A, 1581:63-70,

Sivakanthan, S., & Madhujith, T. (2020). Current trends in applications of enzymatic interesterification of fats and oils: A review. Lwt, 132:109880,

Soares, F. A. S. D. M., da Silva, R. C., da Silva, K. C. G., Lourenço, M. B., Soares, D. F., & Gioielli, L. A. (2009). Effects of chemical interesterification on physicochemical properties of blends of palm stearin and palm olein. Food research international, 42:1287-1294,

Sprague, J. M., Beckham, L. J., & Adkins, H. (1934). Preparation of 1, 3-diketones by the claisen reaction. Journal of the American Chemical Society, 56:2665-2668,

Tan, C.-P., & Nehdi, I. A. (2012). 'The physicochemical properties of palm oil and its components.' In, *Palm oil* (pp. 377-391). Elsevier.

Wen, C., Shen, M., Liu, G., Liu, X., Liang, L., Li, Y., . . . Xu, X. (2023). Edible vegetable oils from oil crops: Preparation, refining, authenticity identification and application. Process Biochemistry, 124:168-179,

Zbikowska, A., Onacik-Gür, S., Kowalska, M., Zbikowska, K., & Feszterová, M. (2023). Trends in Fat Modifications Enabling Alternative Partially Hydrogenated Fat Products Proposed for Advanced Application. Gels, 9:453,

Zhang, Z., Ye, J., Lee, W. J., Akoh, C. C., Li, A., & Wang, Y. (2021). Modification of palm-based oil blend via interesterification: Physicochemical properties, crystallization behaviors and oxidative stabilities. Food Chemistry, 347:129070,

Figure caption

Figure 1: Evolution of the melting profile of IE and NIE POSt:HOSO blends

(a) POSt:HOSO (30:70 %w/w)

(b) POSt:HOSO (50:50 %w/w)

(c) POSt:HOSO (70:30 %w/w)

NIE: Non interesterified

CIE: Chemical interesterification

Figure 2: Evolution of the melting profile of IE and NIE of HOPO-based blends

(a) HOPSt:HOPO (30:70 %w/w)

(b) HOPSt:HOPO (50:50 %w/w)

(c) POSt:HOPO (50:50 %w/w)

(d) PKSt:HOPO (50:50 %w/w)

NIE: Non interesterified

CIE: Chemical interesterification

Figure 3: Production of DAKs function of delta area of the different blends

Figure 1

(a)

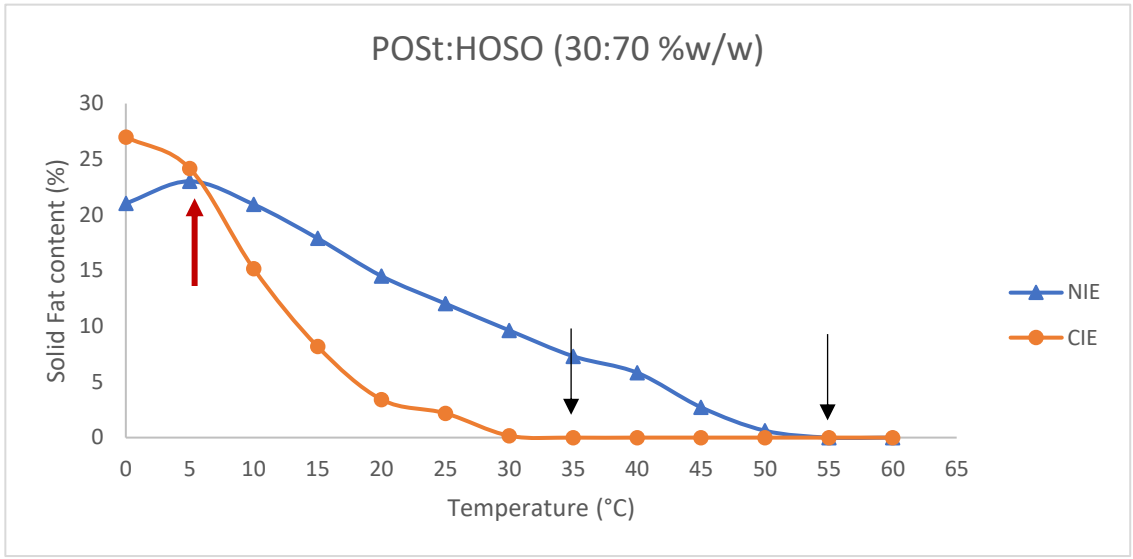
POSt:HOSO (30:70 %w/w)
Solid Fat content (%)
Temperature (°C)
NIE
CIE

(b)

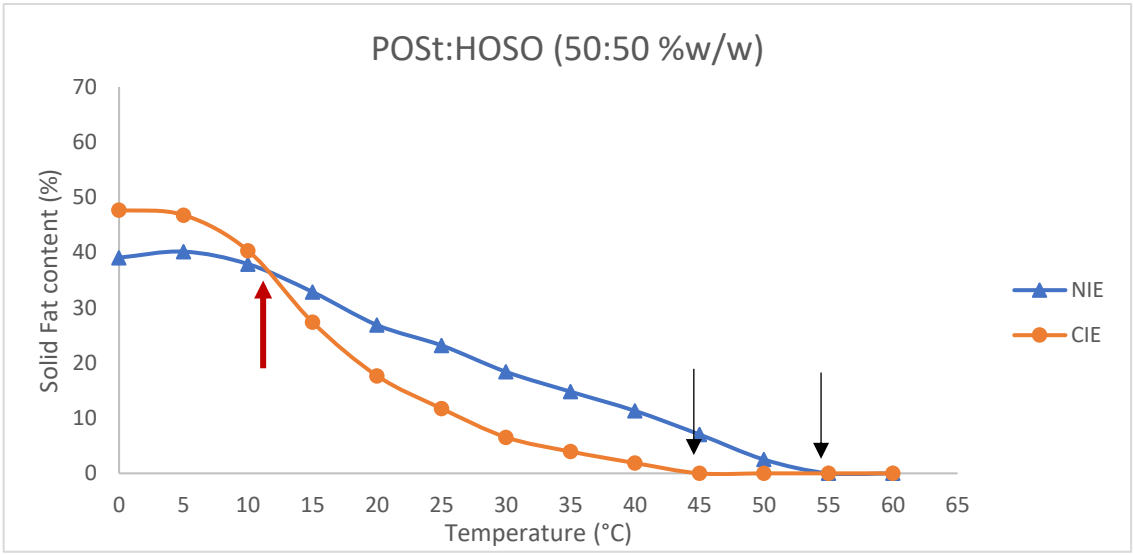
POSt:HOSO (50:50 %w/w)
Solid Fat content (%)
Temperature (°C)
NIE
CIE

(c)

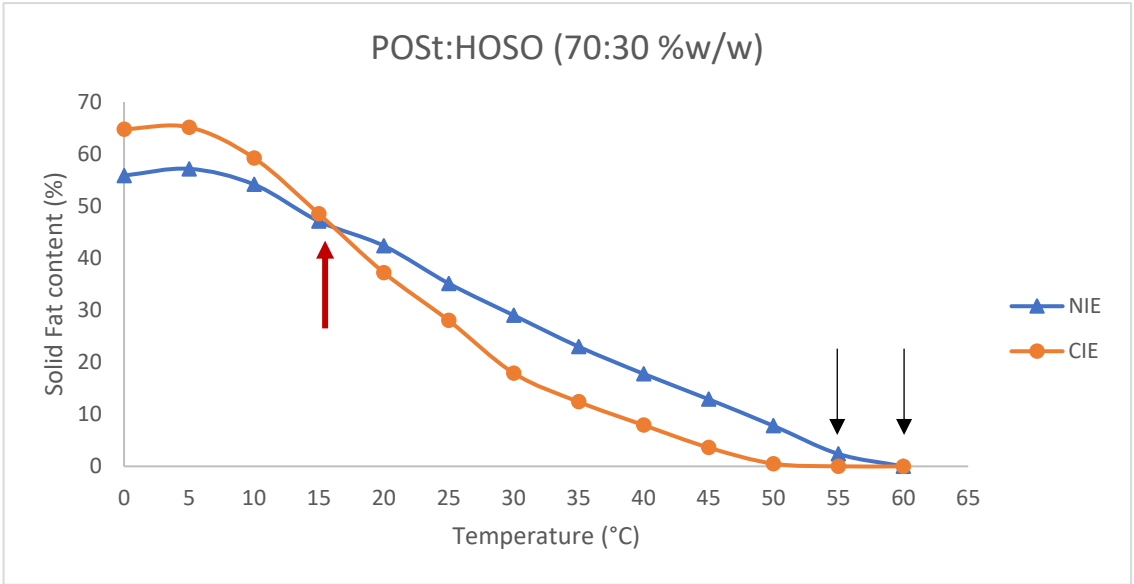
POSt:HOSO (70:30 %w/w)
Solid Fat content (%)
Temperature (°C)
NIE
CIE

Figure 2

(a)

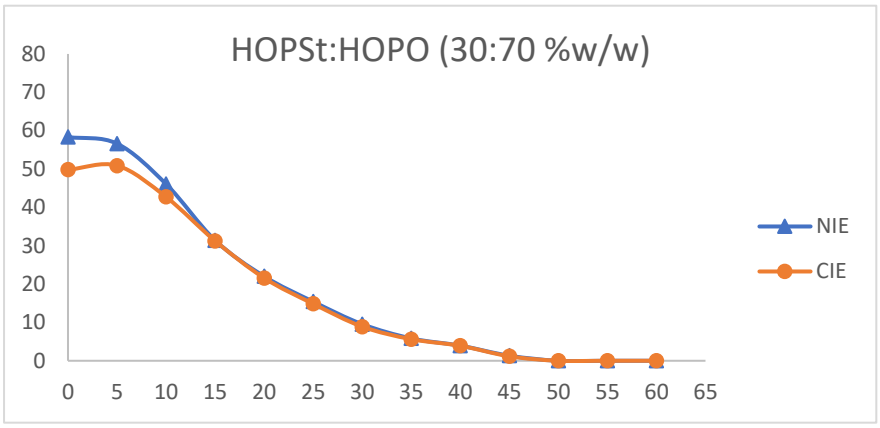

(b)

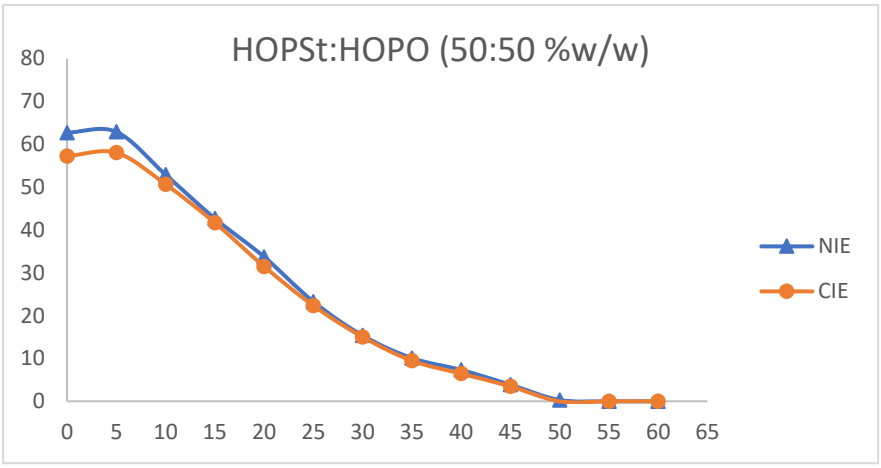

(c)

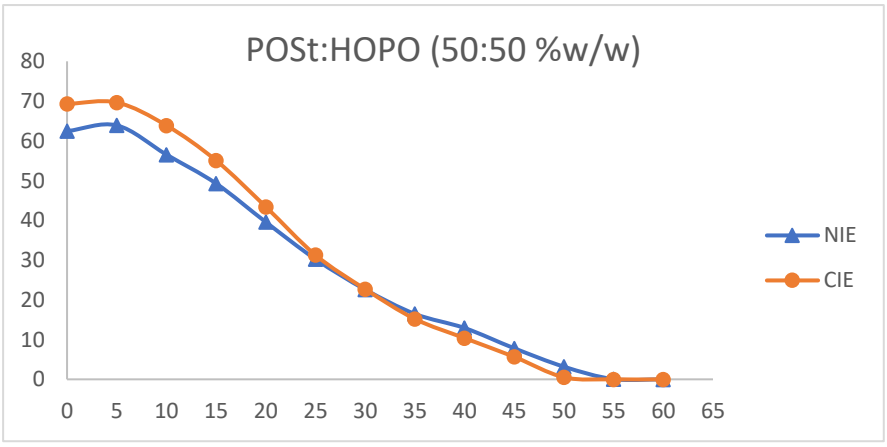

(d)

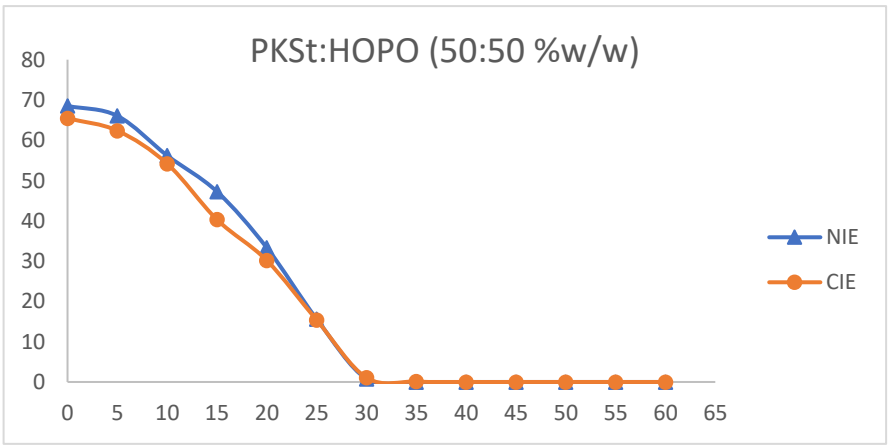

Figure 3

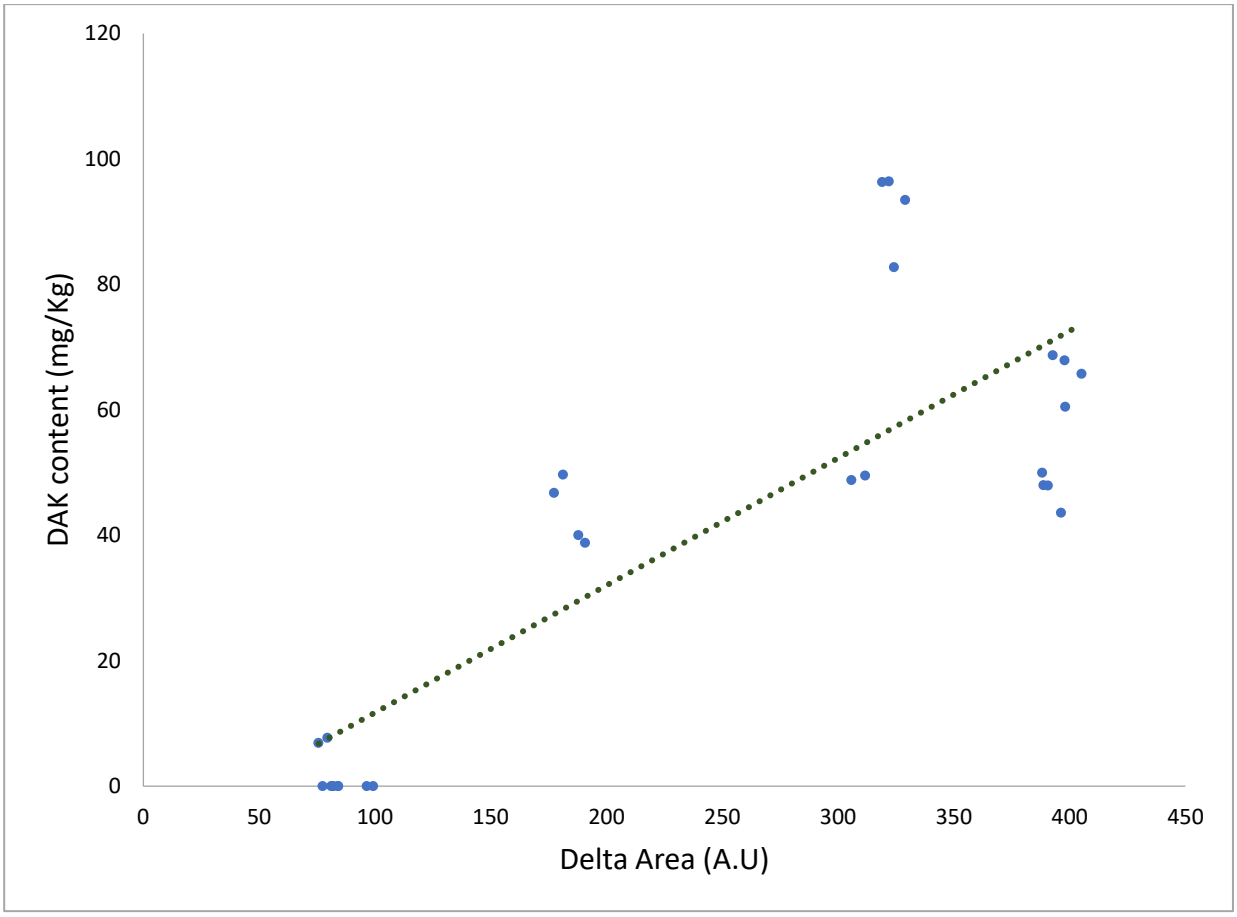
120
100
80
60
40
20
0
DAK content (mg/Kg)
0
50
100
150
200
250
300
350
400
450
Delta Area (A.U)

Table 1: Fatty acids composition

Compounds	HOPSt/HOPO 30/70	HOPSt/HOPO 50/50	PKSt/HOPO 50/50	POSt/HOPO 50/50	POSt/HOSO 30/70	POSt/HOSO 50/50	POSt/HOSO 70/30
C8	0,01 ± 0.00	0,01 ± 0.00	0,47 ± 0.00	0,01 ± 0.00	0,00 ± 0.00	0,01 ± 0.00	0,01 ± 0.00
C10	0,01 ± 0.00	0,01 ± 0.00	0,95 ± 0.00	0,01 ± 0.00	0,00 ± 0.00	0,01 ± 0.00	0,01± 0.00
C12	0,17 ± 0.01	0,20 ± 0.00	25,50 ± 0.32	0,16 ± 0.02	0,05 ± 0.00	0,08 ± 0.00	0,11± 0.00
C14	0,48 ± 0.01	0,56 ± 0.01	11,82 ± 0.22	0,74 ± 0.02	0,33 ± 0.01	0,54 ± 0.02	0,72 ± 0.02
C16	37,71 ± 0.13	42,08 ± 0.15	21,51 ± 0.22	45,30 ± 0.15	20,51 ± 0.32	31,76 ± 0.15	42,52 ± 1.29
C16:1	0,32 ± 0.00	0,32 ± 0.01	0,19 ± 0.01	0,28 ± 0.00	0,17 ± 0.00	0,18 ± 0.00	0,18 ± 0.00
C18	3,50 ± 0.09	3,55 ± 0.13	2,57 ± 0.00	4,06 ± 0.01	3,49 ± 0.01	3,96 ± 0.02	4,42 ± 0.05
C18:1	47,23 ± 0.19	43,75 ± 0.11	30,22 ± 0.29	40,30 ± 0.14	67,62 ± 0.31	56,04 ± 0.00	45,03 ± 1.22
C18:2	9,48 ± 0.06	8,47 ± 0.11	6,04 ± 0.04	8,14 ± 0.25	6,24 ± 0.02	6,05 ± 0.08	5,82 ± 0.12
C18:3	0,35 ± 0.00	0,31 ± 0.02	0,22 ± 0.00	0,28 ± 0.00	0,10 ± 0.00	0,11 ± 0.01	0,13 ± 0.01
C20	0,28 ± 0.00	0,27 ± 0.00	0,17 ± 0.00	0,30 ± 0.01	0,28 ± 0.01	0,29 ± 0.00	0,31 ± 0.01
C20:1	0,12 ± 0.00	0,11 ± 0.00	0,09 ± 0.00	0,11 ± 0.00	0,20 ± 0.00	0,17 ± 0.00	0,14 ± 0.00
UNSAFA (%)	57.50 ± 0.25	52.96 ± 0.25	36.76 ± 0.34	49.11 ± 0.39	74.33 ± 0.33	62.55 ± 0.09	51.30 ± 1.35
SAFA (%)	42.16 ± 0.24	46.68 ± 0.29	62.99 ± 0.76	50.58 ± 0.21	24.66 ± 0.35	36.65 ± 0.19	48.10 ± 1.37

UNAFA: Unsaturated fatty acids; SAFA: Saturated fatty acids

Table 2: Comparison of the DAKs content in different POSt:HOSO- based samples

	POSt:HOSO 30:70			POSt:HOSO 50:50			POSt:HOSO 70:30		
	NIE	**EIE**	**CIE**	**NIE**	**EIE**	**CIE**	**NIE**	**EIE**	**CIE**
C16:0 – C16:0	-	-	< LOQ	-	-	-	-	-	14.63 ± 0.94
C16:0 – C18:1	-	-	35.26 ± 2.21	-	-	22.19 ± 3.14	-	-	33.21 ± 1.83
C16:0 – C18:0	-	-	< LOQ	-	-	-	-	-	-
C18:1 – C18:1	-	-	56.96 ± 4.28	-	-	25.17 ± 4.89	-	-	17.85 ± 0.96
C18:0 – C18:1	-	-	< LOQ	-	-	< LOQ	-	-	-
C18:1 – C20:0	-	-	-	-	-	-	-	-	-
C18:0 – C20:0	-	-	-	-	-	-	-	-	-
TOTAL	-	-	92.22 ± 6.48	-	-	47.36 ± 2.69	-	-	65.69 ± 3.69
Δ Area			328			402			433

LOQ: Limit of quantification

Table 3: Comparison of the DAKs content in different HOPO- based samples

	HOPSt:HOPO 30:70			HOPSt:HOPO 50:50			POSt:HOPO 50:50			PKSt:HOPO 50:50		
	NIE	**EIE**	**CIE**	**NIE**	**EIE**	**CIE**	**NIE**	**EIE**	**CIE**	**NIE**	**EIE**	**CIE**
C16:0 – C16:0	-	-	-	-	-	-	-	-	10.14 ± 0.14	-	-	-
C16:0 – C18:1	-	-	7.29 ± 0.57-	-	-	-	-	-	20.60 ± 0.28	-	-	-
C16:0 – C18:0	-	-	-	-	-	-	-	-	-	-	-	-
C18:1 – C18:1	-	-	-	-	-	-	-	-	9.68 ± 0.13	-	-	-
C18:0 – C18:1	-	-	-	-	-	-	-	-	-	-	-	-
C18:1 – C20:0	-	-	-	-	-	-	-	-	-	-	-	-
C18:0 – C20:0	-	-	-	-	-	-	-	-	-	-	-	-
TOTAL	-	-	7.29 ± 0.57	-	-	-	-	-	40.43 ± 0.56	-	-	-
Δ Area			78			46			136			62